



CONTROL OF COMBUSTION INSTABILITIES BY A SECOND HEAT SOURCE

Jingxuan Li, Aimee S.Morgans

Department of Aeronautics, Imperial College London, London, UK, SW7 2AZ

email: jingxuan.li@imperial.ac.uk

Lean premixed combustion chambers are susceptible to combustion instabilities arising from the coupling between the heat release rate perturbations and the acoustic disturbances. These instabilities are generally harmful. A second heat source equipped downstream of the unsteady flame can be used to interrupt the coupling between the acoustic waves and unsteady heat release and prevent or suppress instability. A low order model of a Rijke tube with weak mean flows is developed comprising a linear acoustic network and simple flame transfer functions. The stabilities of the system without controller are investigated by varying the time delay and gain of flame model, the flame locations and the temperature jump ratio across the flame. The changes of eigenvalue trajectories due to the presence of the second heater are also discussed by changing the location and flame model of the second heater. It is shown that the second heater can be used to reduce the growth rate of the system and suppress the instabilities.

1. Introduction

Combustion instabilities arise due to the coupling between the unstable combustion process and acoustic disturbances within the combustion chamber [1]. The mechanism can be briefly described as: acoustic noise with a broad frequency bandwidth is produced during the combustion process [2]. These sound waves propagate inside the combustion chamber, interact with the boundaries and return back to the combustion zone with a time delay that depends on the size of the combustion chamber, disturbances of speed of sound and impedances at the boundaries of the combustion chamber. These pressure oscillations generate in turn perturbations of the flow field by modifying the local flowrate, reactant composition or thermodynamic properties in the flame region, producing heat release rate disturbances [1]. When these disturbances are synchronised, they amplify leading to an increase of acoustic energy in the system and a resonance is generally observed at specific tones. These self-sustained instabilities are more likely to happen in lean premixed combustion systems, which offer the potential for reducing NO_x emissions in modern gas turbine design [3].

A second heat source equipped downstream of the unsteady flame can be used to suppress the instabilities of the system. The objective of this paper is to show the effects of parameters of flame model and the location of the second heater on the stabilities of the system. The rest of the paper is organized as follows. The acoustic network without controller and the linear flame model are presented in Section 2. A governing equation is derived to link the linear acoustic response of the

Rijke tube with the flame model. The stabilities of the system without controller are investigated by varying the time delay and gain of flame model, the flame locations and the temperature jump ratio across the flame. The changes of eigenvalue trajectories due to the presence of the second heater are also discussed by changing the location and flame model of the second heater, which are shown in Section 3. The simulation can also be implemented using our open source [8] (OSCILOS) which is freely available (see <http://www.oscilos.com/>). Conclusions are drawn in the final section.

2. Model of combustor without controller

Analysis is carried out on a simple model combustion chamber which consists of a cylindrical Rijke tube with both ends open to the atmosphere. Denoting the distance along the tube axis by the vector x , the inlet and outlet of the tube are at $x = 0$ and $x = l$ respectively. The combustor consists N modules. The inlet and outlet of module k , $1 \leq k \leq N$, are located at $x = x_{k-1}$ and $x = x_k$, respectively. In the analysis, the following assumptions are implemented: (1) The envisaged frequencies are assumed sufficiently small to consider the combustion zone to be “compact” compared to the acoustic wavelength and to only take into account the longitudinal waves. (2) The fluids within the combustor are assumed to be perfect gases. (3) The dissipation of acoustic waves throughout the tube is negligible and acoustic damping only happens at the ends of the tube. (4) There is no noise produced by the entropy waves formed during the unstable combustion process — these waves are assumed to leave the tube without interaction with the flow at the end of tube. (5) The flame is assumed to be always stabilised at the burner outlet. Flame intrinsic instabilities [4] and irregular response to strong disturbances [5], which may cause that the final state of the unstable system is not a limit cycle [6], have not been accounted for in this work. (6) The specific heat capacity ratio is considered as a constant $\gamma = 1.4$ and does not change with temperature and compositions of gases. (7) The mean flow is weak and negligible, which enables the simplification of the jump equations across the interface connecting two modules, e.g., the jump equations across the flame for a Rijke tube can be written as [7]:

$$(1) \quad \tilde{p}_2(x_{f1}, s) = \tilde{p}_1(x_{f1}, s)$$

$$(2) \quad \tilde{u}_2(x_{f1}, s) = \tilde{u}_1(x_{f1}, s) + \frac{\gamma - 1}{\bar{\rho}\bar{c}^2} \tilde{q}_1(s)$$

where p , u , ρ , c and \dot{q}_1 denotes the pressure, velocity, speed of sound and heat release rate per surface area, respectively. x_{f1} specifies the location of the flame. The superscripts $\bar{\cdot}$ and $\tilde{\cdot}$ indicate the mean value and the Laplace transform, respectively. $s = \sigma + i2\pi f$ represents the Laplace variable, σ is the growth rate and f denotes the frequency. For weak flows, the mean pressures in every module are the same. $\bar{\rho}_1\bar{c}_1^2 = \bar{\rho}_2\bar{c}_2^2 = \dots = \gamma\bar{p}$.

A flame transfer function \mathcal{T}_1 can be used to describe the response of heat released from the unsteady flame to oncoming weak perturbed flows, which can be mathematically expressed as:

$$(3) \quad \frac{\tilde{\dot{q}}}{\tilde{q}} = \mathcal{T}_1 \frac{\tilde{u}_1}{\tilde{u}_1}$$

Theoretical models have been devised to analytically describe the transfer function [8]. For example, the G-equation model obtains the flame shape by using a kinematic model for the flame position response to oncoming velocity perturbations, and has been studied for various flame shapes: conical, V-shape, M-shape and matrix flames, with their detailed derivations collected in Lieuwen’s book [9]. Assuming the mean heat release rate per unit surface area to be $\bar{\dot{q}} = \bar{\rho}_1\bar{u}_1C_p(\bar{T}_2 - \bar{T}_1)$ [7, 8] and C_p to be constant for the temperature band envisaged in this paper, it is thus possible to substitute the flame

model into Eq. 2 to give:

$$(4) \quad \tilde{u}_2(x_{f1}, s) = \left(1 + \left(\frac{\bar{T}_2}{\bar{T}_1} - 1 \right) \mathcal{T}_1 \right) \tilde{u}_1(x_{f1}, s)$$

The acoustic field within the combustor can be described as the summation of forward and backward propagating plane waves. According to the linear acoustic theory, all flow and thermodynamic variables can be decomposed into a mean value and an acoustic perturbation, which is assumed to be small compared to the corresponding mean value. Considering acoustic waves propagating in both directions, the pressure and velocity perturbations in module k can be expressed as:

$$(5) \quad \tilde{p}_k(x, s) = \tilde{A}_k^+(s) \exp(-\tau_k s) + \tilde{A}_k^-(s) \exp(\tau_k s)$$

$$(6) \quad \tilde{u}_k(x, s) = \frac{1}{\bar{\rho}_k \bar{c}_k} \left(\tilde{A}_k^+(s) \exp(-\tau_k s) - \tilde{A}_k^-(s) \exp(\tau_k s) \right)$$

where $\tilde{A}_k^+(s)$ and $\tilde{A}_k^-(s)$ denote the amplitude of the downstream and upstream propagating acoustic waves respectively. $\tau_k = x_k/\bar{c}_k$ represents the propagation time of sound in module k . By substituting Eqs. 5 and 6 into Eqs. 1 and 4, one can get the governing equations linking the acoustic waves at the two sides of the flame:

$$(7) \quad \tilde{A}_2^+(s) + \tilde{A}_2^-(s) = \tilde{A}_1^+(s) \exp(-\tau_1 s) + \tilde{A}_1^-(s) \exp(\tau_1 s)$$

$$(8) \quad \tilde{A}_2^+(s) - \tilde{A}_2^-(s) = \frac{\bar{c}_1}{\bar{c}_2} \left(1 + \left(\frac{\bar{T}_2}{\bar{T}_1} - 1 \right) \mathcal{T}_1 \right) \left(\tilde{A}_1^+(s) \exp(-\tau_1 s) - \tilde{A}_1^-(s) \exp(\tau_1 s) \right)$$

The link between the outward and inward propagating waves at the end of the combustor can be described by the reflection coefficients. When the indirect noise induced by the entropy waves can be neglected, the pressure reflection coefficients at the inlet and outlet are characterized by R_1 and R_2 respectively:

$$(9) \quad \tilde{A}_1^+(s) = R_1 \tilde{A}_1^-(s)$$

$$(10) \quad \tilde{A}_N^-(s) = R_2 \tilde{A}_N^+(s) \exp(-2\tau_N s)$$

By substituting the above boundary conditions into Eqs. 7 and 8, one is left with:

$$(11) \quad R_1 R_2 - \exp\left(2(\tau_1 + \tau_2)s\right) + \frac{\alpha_1 - 1}{\alpha_1 + 1} \left(R_1 \exp(2\tau_2 s) - R_2 \exp(2\tau_1 s) \right) = 0$$

where,

$$(12) \quad \alpha_1 = \frac{\bar{c}_1}{\bar{c}_2} \left(1 + \left(\frac{\bar{T}_2}{\bar{T}_1} - 1 \right) \mathcal{T}_1 \right)$$

The eigenvalues can be obtained by solving Eq. 11. When there is no heat addition, $\alpha_1 = 1$, the third component of Eq. 11 equals to zero and Eq. 11 is simplified to:

$$(13) \quad R_1 R_2 - \exp\left(2(\tau_1 + \tau_2)s\right) = 0$$

Table 1: Parameters used in the analysis. They are fixed unless otherwise stated. \bar{T}_1 always equals to 300 K.

γ [-]	R_g [J kg ⁻¹ K ⁻¹]	\bar{T}_1 [K]	\bar{T}_2 [K]	l [m]	R_1 [-]	R_2 [-]
1.4	287	300	600	1	-1	-1

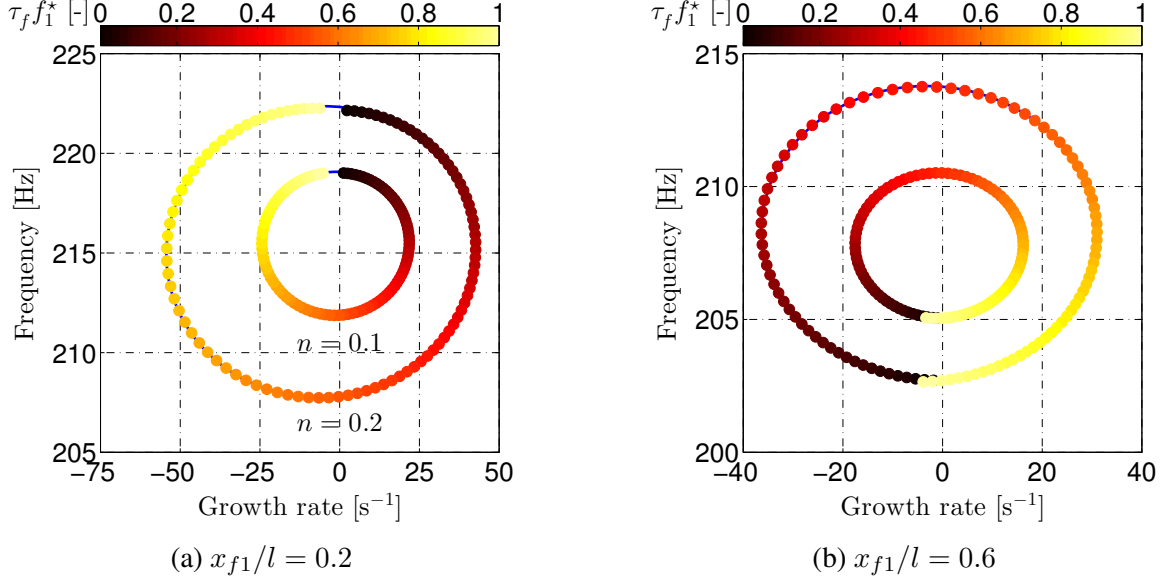


Figure 1: Evolutions of eigenfrequency of first mode with corresponding growth rate for different time delay τ_{f1} and different flame location x_{f1} . The time delay τ_{f1} ranges from 0 to $1/f_1^*$. $f_1^* = 1/(2(\tau_1 + \tau_2))$. The blue solid lines indicate the approximated ellipses of the trajectories.

The growth rate of the eigenvalue equals to:

$$(14) \quad \sigma = \ln |R_1 R_2|$$

The growth rate is always no-positive because the absolute value of the pressure reflection coefficient cannot be larger than unit. The acoustic energy does not increase without any external acoustic source at the boundary. The presence of the heat addition that enables the system to be unstable.

We now consider the situation with mean heat addition and heat fluctuations. For sake of simplicity, the famous $n - \tau$ model is used as the flame transfer function, which can be expressed as:

$$(15) \quad \mathcal{T}_1(s) = n_1 \exp(-\tau_{f1}s)$$

where, n_1 and τ_{f1} denotes the gain and time delay of the transfer function. The gain, specifying the amplification effect of the flame on the incident acoustic flow perturbations, features the shape of low-pass filter and is cut-off at a certain frequency related to the shape of the steady flame and other properties. The time delay, also represented as the time lag of heat release perturbations with respect to oncoming flow perturbations, in particular for premixed flames, is considered to be proportional to the length of steady flame. For example, the time delay τ_{f1} of the laminar conical premixed flame is equal to $H/3\bar{u}_1$ for lower frequency band and increases with frequency, while the V-shape flame features a constant time delay of $2H/3\bar{u}_1$, where H specifies the height of the flame.

We first consider a Rijke tube with its major geometry parameters and thermal properties described in Table 1. By keeping the gain of flame model constant, it is possible to examine the evolution of eigenvalues with increasing the time delay. Figure 1 shows the trajectories of the first mode of Rijke tube with time delay τ_{f1} ranging from 0 to $1/f_1^*$, for different gain of flame model and different flame locations. We can find that the trajectory features a periodic motion and $f_1^* = 1/(2(\tau_1 + \tau_2))$ can be

used as an estimation of the time period. For a small gain n_1 , the trajectory features a shape of ellipse and can be approximately expressed as:

$$(16) \quad \frac{(f - f_1^0)^2}{(f_1^1)^2} + \frac{(\sigma - \sigma_1^0)^2}{(\sigma_1^1)^2} = 1$$

where the point $[f_1^0, \sigma_1^0]$ denotes the center of the ellipse. f_1^1 and σ_1^1 represent the amplitudes of frequency change and growth rate change, respectively. The value σ_1^1 can also be used to evaluate the stability of the system. If σ_1^1 has a larger value, the system may become very unstable for a time delay range. It is more difficult to control the combustion instabilities for these situations. While for a smaller σ_1^1 , a simple attached damping device is sufficient to ensure the stability of the system. It is interesting to examine the change of the ellipse with the flame location, by successively varying the flame position ratio x_{f1}/l , e.g., the results are shown in figures 2 and 3. When the flame position ratio x_{f1}/l is increased, more cold gases occupy the Rijke tube and the mean eigenfrequency $f_{1,0}$ decreases. The mean eigenfrequency can also be evaluated by the solution of the simplified equation:

$$(17) \quad R_1 R_2 - \exp\left(2(\tau_1 + \tau_2)s\right) - \frac{\bar{c}_2 - \bar{c}_1}{\bar{c}_2 + \bar{c}_1} \left(R_1 \exp(2\tau_2 s) - R_2 \exp(2\tau_1 s) \right) = 0$$

This equation can be further simplified when $R_1 = R_2 = -1$, which is written as:

$$(18) \quad \sin\left(2\pi(\tau_1 + \tau_2)f\right) - \frac{\bar{c}_2 - \bar{c}_1}{\bar{c}_2 + \bar{c}_1} \sin\left(2\pi(\tau_2 - \tau_1)f\right) = 0$$

Fig. 2(a) shows the evolutions of f_1^0 (markers) and their predictions from Eq. 18 (cyan solid lines). The two results match well for the envisaged cases. One may also roughly predict the mean eigenfrequency using the simple equation $f_1^* = 1/(2(\tau_1 + \tau_2))$, which is for example represented by the dashed green lines in Fig. 2(a). The variation of eigenfrequency is evaluated by $f_{1,1}$, e.g., the results are shown in Fig. 2(b). The value of $f_{1,1}$ equals to zero at the two boundaries. When the flame is placed at the position where $\tau_1 \approx \tau_2$, the variations of eigenfrequency $f_{1,1}$ and growth rate $\sigma_{1,1}$ always equal to zero. The unsteady flame has no effect on the stability of the system at this position. One denotes this position as x_{f1}^* . From Fig. 3(a), we also find that the mean growth rate $\sigma_{1,0}$ approaches $\ln|R_1 R_2|$ for weak gain of flame transfer function. When $R_1 = R_2 = -1$, $\sigma_{1,0}$ approaches zero. We may also find that when the flame position is at the left side of x_{f1}^* , the growth rate of the

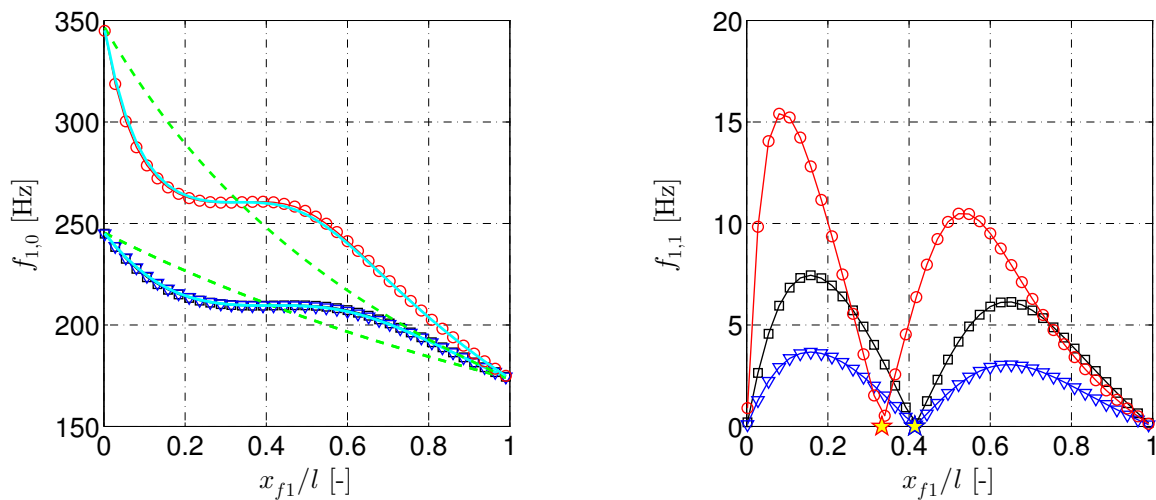


Figure 2: Evolution of f_1^0 and f_1^1 with the flame location for different temperature ratio \bar{T}_2/\bar{T}_1 and gain of flame transfer function n_1 . Markers ∇ : $\bar{T}_2/\bar{T}_1 = 2$ and $n_1 = 0.1$. Markers \square : $\bar{T}_2/\bar{T}_1 = 2$ and $n_1 = 0.2$. Markers \circ : $\bar{T}_2/\bar{T}_1 = 4$ and $n_1 = 0.1$. Yellow Stars: $\tau_1 = \tau_2$. Dashed green line: f_1^* .

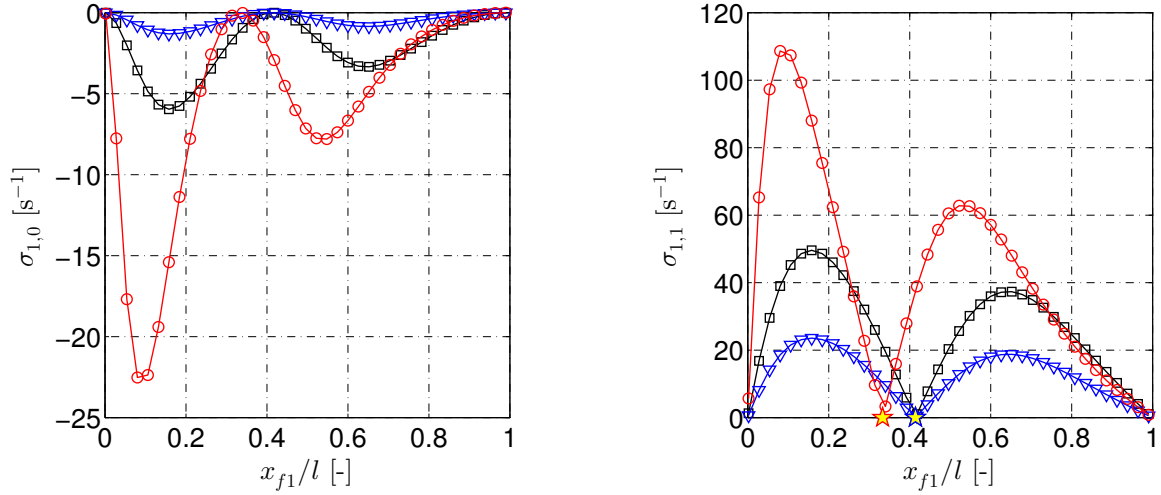


Figure 3: Evolution of σ_1^0 and σ_1^1 with the flame location for different temperature ratio \bar{T}_2/\bar{T}_1 and gain of flame transfer function n_1 . Markers ∇ : $\bar{T}_2/\bar{T}_1 = 2$ and $n_1 = 0.1$. Markers \square : $\bar{T}_2/\bar{T}_1 = 2$ and $n_1 = 0.2$. Markers \circ : $\bar{T}_2/\bar{T}_1 = 4$ and $n_1 = 0.1$. Yellow Stars: $\tau_1 = \tau_2$.

first mode increases to positive when τ_{f1} is increased from zero to $1/(2f_1^*)$ and the flame is unstable. The variation of growth rate $\sigma_{1,1}$ increases when the flame position x_{f1} is increased from zero to x_{f1}^* . The growth rate reaches the maximum value when $x_{f1} \approx x_{f1}^*/2$ and then decreases to zero when $x_{f1} = x_{f1}^*$. When the flame is located after this key position x_{f1}^* , the growth rate decreases when τ_{f1} is increased from zero to $1/(2f_1^*)$.

3. Model of combustor with controller

We now equip a second heat source downstream of the first one. The location of the heater is $x = x_{f2}$. The second heater may not produce enough mean heat release to change the mean temperature, but can bring heat release rate perturbations. The mean temperatures before and after the second heat source are considered the same. The heat release rate can be linked with the velocity perturbations by the following model used in [10]:

$$(19) \quad \tilde{q}_2(s) = \frac{\sqrt{3}}{4} K \tilde{u}_2(s) \exp(-\tau_{f2}s)$$

where K denotes the strength of the heater and τ_{f2} indicates the time delay of the model. The jump equations across this heater can thus be expressed as:

$$(20) \quad \tilde{p}_3(x_{f2}, s) = \tilde{p}_2(x_{f2}, s)$$

$$(21) \quad \tilde{u}_3(x_{f2}, s) = \tilde{u}_2(x_{f2}, s) + \frac{\gamma - 1}{\rho \bar{c}^2} \tilde{q}_2(s) = (1 + \alpha_2) \tilde{u}_2(x_{f2}, s)$$

where α_2 specifies the heat release rate model and can also be expressed as a gain n_2 and a time delay τ_{f2} :

$$(22) \quad \alpha_2 = n_2 \exp(-\tau_{f2}s) = \frac{\gamma - 1}{\gamma \bar{p}} \frac{\sqrt{3}}{4} K \exp(-\tau_{f2}s)$$

It is then possible to obtain the governing equation, which can be mathematically expressed as:

$$(23) \quad \left(\frac{\alpha_1 - 1}{\alpha_1 + 1} R_1 - \exp(2\tau_1 s) \right) \left(\exp(2\tau_3 s) + \frac{\alpha_2}{\alpha_2 + 2} R_2 \right) \exp(2\tau_2 s) \\ + \left(R_1 - \frac{\alpha_1 - 1}{\alpha_1 + 1} \exp(2\tau_1 s) \right) \left(\frac{\alpha_2}{\alpha_2 + 2} \exp(2\tau_3 s) + R_2 \right) = 0$$

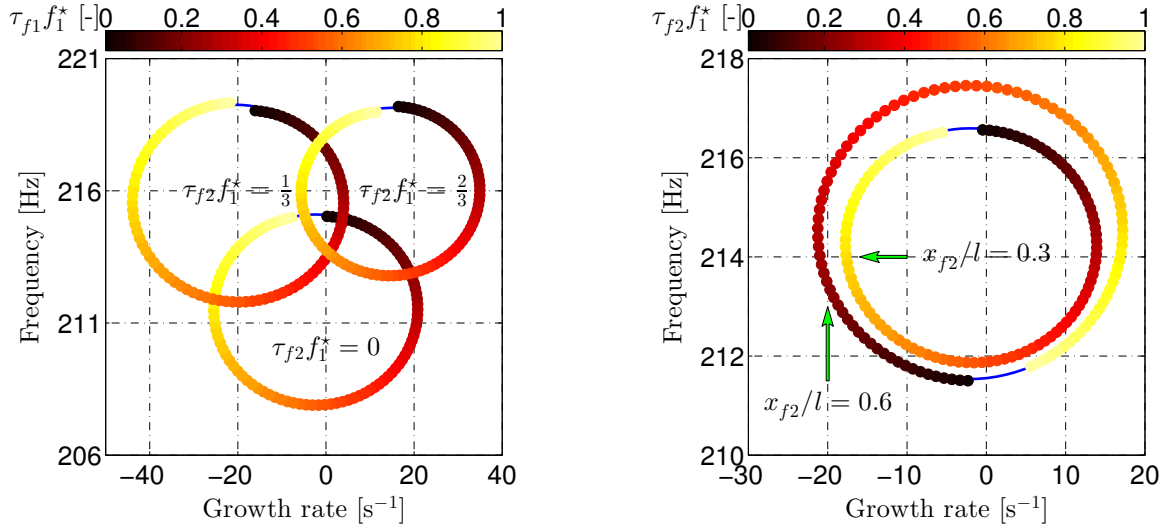


Figure 4: Left figure: trajectories of eigenvalues for different τ_{f_2} when $x_{f_2}/l = 0.6$. Right figure: trajectories of the center of ellipse with τ_{f_2} for two locations. $x_{f_1}/2 = 0.2$. $n_1 = 0.1$ and $n_2 = 0.1$.

We now consider an unstable case, where the location of the first heat source is $x_{f_1}/l = 0.2$ and the gain is $n_1 = 0.1$, e.g., the results are shown in figures 4 and 5. When the second heat source is placed at the location $x_{f_2}/l = 0.6$, the trajectories of eigenvalues change with the time delay τ_{f_2} . It is interesting to find that the diameters of the trajectories are nearly constant for smaller n_2 , and the center of the trajectory $[f_1^0, \sigma_1^0]$ also rotates on a ellipse path with increasing τ_{f_2} . The trajectory of the center can be approximately expressed as:

$$(24) \quad \frac{(f_1^0 - \hat{f}_1^0)^2}{(\hat{f}_1^1)^2} + \frac{(\sigma_1^0 - \hat{\sigma}_1^0)^2}{(\hat{\sigma}_1^1)^2} = 1$$

where the point $[\hat{f}_1^0, \hat{\sigma}_1^0]$ denotes the center of the new ellipse. \hat{f}_1^1 and $\hat{\sigma}_1^1$ represent the amplitudes of frequency change and growth rate change due to the presence of second heater, respectively. $\hat{\sigma}_1^1$ can also be used to evaluate the performance of the controller. When $\hat{\sigma}_1^1$ has a larger value, the entire growth rate can be largely reduced by adjusting the time delay of the second heater τ_{f_2} to a suitable value.

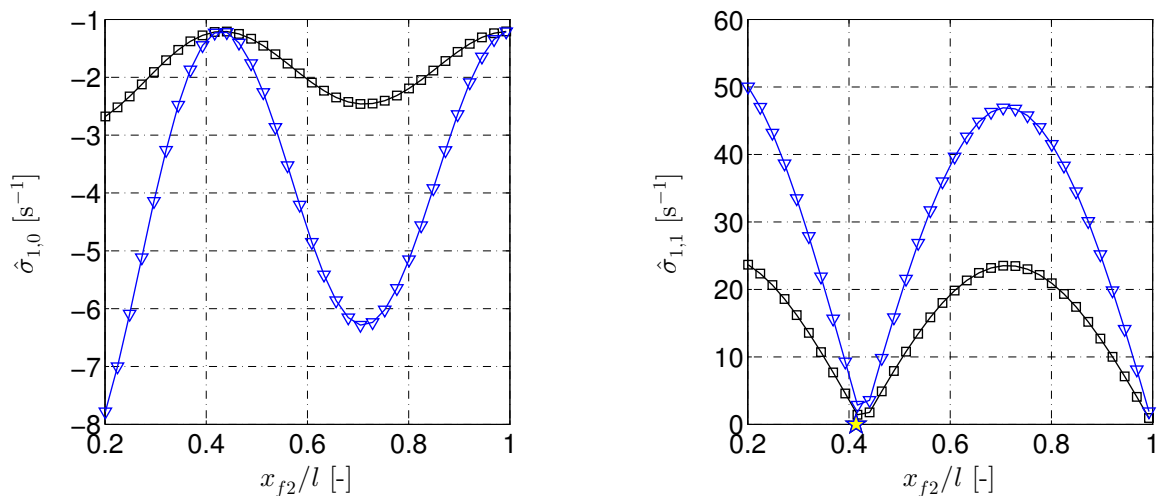


Figure 5: Evolutions of $\hat{\sigma}_1^0$ and $\hat{\sigma}_1^1$ with the second flame location for different gain of flame transfer function n_2 . Markers ∇ : $n_1 = 0.2$. Markers \square : $n_1 = 0.1$. Yellow Stars: $\tau_1 = \tau_2$.

It is possible to examine the change of the new ellipse with the location of the second heat source. Figure 5 shows the evolutions of $\hat{\sigma}_1^0$ and $\hat{\sigma}_1^1$ with x_{f2}/l . The trajectories of $\hat{\sigma}_1^1$ has a similar shape of σ_1^1 (see Fig. 3(b)). To achieve a good control, it is better to place the second heater near the position of $x_{f2}/l = (1 - x_{f1}^*/l)/2$. The entire growth rate is reduced when $0 \leq \tau_{f2}f_1^* \leq 0.5$. The control performance can be enhanced by increasing the gain n_2 .

4. Conclusions

This article has presented a new control strategy of combustion instabilities, which employs a second heat source downstream of the unsteady flame within the combustor. A low order model of a Rijke tube with weak mean flows has been developed comprising a linear acoustic network and simple flame transfer functions. The stabilities of the system without and with controller have been investigated by varying the time delay and gain of flame model, the flame locations and the temperature jump ratio across the flame. It was shown that the trajectory of the eigenvalues with time delay of flame model features a shape of ellipse for a weak gain of flame model. The diameters of the ellipse change with the gain and flame locations. Results showed that by using a proper second heater, the growth rate of the system can be reduced and the instabilities can be suppressed and controlled.

Acknowledgement

The authors would like to gratefully acknowledge the European Research Council (ERC) Starting Grant ACOULOMODE (2013-2018) for supporting the current research.

References

1. Candel, S. Combustion dynamics and control: Progress and challenges. *Proceedings of the Combustion Institute*, **29** (1), 1–28, (2002).
2. Mahan, J. R. and Karchemer, A. *Aeroacoustics of Flight Vehicles: Theory and Practice. Volume 1: Noise Sources*, volume 1, chapter Combustion and core noise, pages 483–517. WRDC Technical Report 90-3052, (1991).
3. Correa, S. M. Power generation and aeropropulsion gas turbines: From combustion science to combustion technology. *Proceedings of the Combustion Institute*, **27** (2), 1793–1807, (1998).
4. Lieuwen, T. Modeling premixed combustion-acoustic wave interactions: A review. *Journal of Propulsion and Power*, **19** (5), 765–781, (2003).
5. Bourehla, A. and Baillot, F. Appearance and stability of a laminar conical premixed flame subjected to an acoustic perturbation. *Combustion and Flame*, **114** (3-4), 303–318, (1998).
6. Boudy, F., Durox, D., Schuller, T., and Candel, S. Analysis of limit cycles sustained by two modes in the flame describing function framework. *Comptes Rendus Mécanique*, **341** (1–2), 181–190, (2013).
7. Dowling, A. P. The calculation of thermoacoustic oscillations. *Journal of Sound and Vibration*, **180** (4), 557–581, (1995).
8. Li, J. and Morgans, A. S. Time domain simulations of nonlinear thermoacoustic behaviour in a simple combustor using a wave-based approach. *Journal of Sound and Vibration*, (0), –, (2015).
9. Lieuwen, T. *Unsteady Combustor Physics*. Cambridge University Press, (2012).
10. Sayadi, T., Chenadec, V. L., Schmid, P. J., Richecoeur, F., and Massot, M. Thermoacoustic instability - a dynamical system and time domain analysis. *Journal of Fluid Mechanics*, **753**, 448–471, (2014).